Reprinted from Biochemistry, 1992, 31.


# Mechanism of Adenylate Kinase. Structural and Functional Roles of the Conserved Arginine-97 and Arginine-132†

Terri Dahnke, Zhengtao Shi, Honggao Yan, Ru-Tai Jiang, and Ming-Daw Tsai*

*Department of Chemistry and Ohio State Biochemistry Program, The Ohio State University, Columbus, Ohio 43210*

*Received January 23, 1992; Revised Manuscript Received April 10, 1992*

ABSTRACT: The structural and functional roles of two conserved active site residues, Arg-97 and Arg-132, in chicken muscle adenylate kinase (AK) were evaluated by site-directed mutagenesis in conjunction with one- and two-dimensional proton nuclear magnetic resonance (NMR), kinetics, and guanidine hydrochloride-induced denaturation. In addition, $^{31}P$ NMR analysis was used to evaluate the contribution of Arg-97 to the phosphorus stereospecificity of AK. The results and conclusions are summarized as follows: (i) Kinetic analysis of R97M reveals 6- and 28-fold increases in the dissociation constant $K_i$ and Michaelis constant $K$ of AMP, respectively, and a moderate 30-fold decrease in $k_{cat}$. The $K_i$ and $K$ values of MgATP are relatively unperturbed. The localized effect of AMP stabilization was independently confirmed by proton NMR titration, which showed a ca. 20-fold increase in the dissociation constant of AMP but not of MgATP. (ii) R132M affords a dramatic decrease in $k_{cat}$ by a factor of $8.0 \times 10^3$, with unchanged dissociation and Michaelis constants for either substrate. The lack of perturbation in the affinities toward substrates was confirmed by proton NMR titration. (iii) Although small chemical shift changes were observed for the free mutants and their complexes with substrates, further analyses by nuclear Overhauser enhanced spectroscopy with the bisubstrate analogue inhibitor, $P^1,P^5$-bis(5′-adenosyl)pentaphosphate ($AP_5A$), indicated little perturbation in the global conformation. (iv) Contributions to conformational stability by Arg-97 and Arg-132 are negligible on the basis of the free energy of unfolding, $\Delta G_d^{H_2O}$. (v) R97M was predicted and demonstrated to exhibit enhanced stereospecificity at the AMP site by at least 10-fold relative to WT in the conversion of adenosine 5′-monothiophosphate to adenosine 5′-(1-thiodiphosphate). This result for R97M was predicted on the basis of the orientation of Arg-97 relative to Arg-44 and AMP in the active site as observed in available crystal structures and the stereospecificity results of R44M [Jiang, R.-T., Dahnke, T., & Tsai, M.-D. (1991) *J. Am. Chem. Soc. 113*, 5485–5486]. (vi) The above structural and functional analyses led us to conclude that Arg-97 interacts with the phosphoryl group of AMP, beginning at the binary complex (1–2 kcal/mol), continuing through the transition state (3.5 kcal/mol), and that Arg-132 stabilizes the transition state by greater than 5 kcal/mol. (vii) The functional importance of Arg-97 appears to be similar to that of Arg-44 [Yan, H., Dahnke, T., Zhou, B., Nakazawa, A., & Tsai, M.-D. (1990) *Biochemistry 29*, 10956–10964]. The results for R97M also clarify conflicting reports from analogous mutants in other types of AK and support conclusions based upon analysis of the mitochondrial matrix AK·AMP crystal structure [Diederichs, K., & Schulz, G. E. (1991) *J. Mol. Biol. 217*, 541–549].

While significant progresses have been made on the structure–function relationship of adenylate kinase (AK)[1,2] as reviewed recently by Tsai and Yan (1991), the functional roles of most active site residues remain to be established. The best characterized region of substrate sites is the phosphate binding region. Crystal structural analyses of the $MgAP_5A$ complexes of yeast AK (AKy) (Egner et al., 1987) and *Escherichia coli* AK (AKe) (Müller & Schulz, 1988) suggest that the phosphates are surrounded by several conserved arginine residues. The structure of the AK1·$MgAP_5A$ complex has not been reported; however, Egner et al. (1987) showed an overlay of the structure of free AK1 with that of AKy·$MgAP_5A$, as shown in Figure 1. The numbering of residues in Figure 1 is according to the "family numbering system" (Schulz et al., 1986); the arginine residues of AK1 addressed in this paper, 44, 97, 132, 138, and 149, correspond to residues 53, 106, 141, 178, and 189, respectively, in the family numbering system. While the structure of AKy·$MgAP_5A$ best represents the current knowledge on the substrate sites of AK, we consider it as a starting point to probe the *quantitative* structure–function relationship of AK.

† This work was supported by a grant from National Science Foundation (DMB-8904727). This study made use of a Bruker AM-500 NMR spectrometer at The Ohio State University, partially funded by NIH Grant RR01458, the National Magnetic Resonance Facility at Madison supported by NIH Grants RR02301 and RR02781 and NSF grant DMB-8415048. This is paper 13 in the series "Mechanism of Adenylate Kinase". For paper 12, see Dahnke et al. (1991).

[1] Abbreviations: ADP, adenosine 5′-diphosphate; ADPαS, adenosine 5′-(1-thiodiphosphate); AK, adenylate kinase; AMP, adenosine 5′-monophosphate; AMPS, adenosine 5′-monothiophosphate; $AP_5A$, $P^1,P^5$-bis(5′-adenosyl)pentaphosphate; ATP, adenosine 5′-triphosphate; ATPαS, adenosine 5′-(1-thiotriphosphate); 1D, one-dimensional; 2D, two-dimensional; CD, circular dichroism; DTT, dithiothreitol; EDTA, ethylenediaminetetraacetate; FID, free induction decay; Gdn-HCl, guanidine hydrochloride; NMR, nuclear magnetic resonance; NOE, nuclear Overhauser effect; NOESY, nuclear Overhauser enhanced spectroscopy; PAGE, polyacrylamide gel electrophoresis; SDS, sodium dodecyl sulfate; Tris, 2-amino-2-(hydroxymethyl)-1,3-propanediol; UV, ultraviolet; WT, wild type.

[2] The AK from different sources are abbreviated as follows: from muscle, AK1 (followed by the letters c, h, p, and r designating chicken, human, porcine, and rabbit, respectively); from *E. coli*, AKe; from yeast, AKy; from mammalian mitochondrial intermembrane space, AK2; from mammalian mitochondrial matrix, AK3. Unless otherwise specified, the numbering system used in this paper is the conventional system for AK1. Although cAK has one additional residue near the N-terminus (Kishi et al., 1986), the Met-1 residue is absent in the cAK expressed in *E. coli* (Tanizawa et al., 1987). This makes numbering of cAK consistent with other AK1.

0006-2960/92/0431-6318$03.00/0 

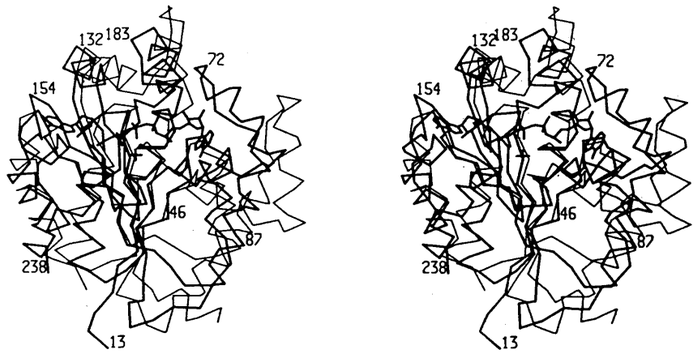


FIGURE 1: Chain fold overlay of free AK1p (thin line) and AKy·MgAP$_5$A (thick line). The adenosines at the left- and right-hand sides correspond to those at the ATP and AMP sites, respectively; + indicates the $Mg^{2+}$ position. The residue numbers are according to the family numbering system (Schulz et al., 1986), which differs from the AK1 numbering used in this paper. Reproduction with permission from Egner et al. (1987) *J. Mol. Biol. 199*, 649–658. Copyright 1987 Academic Press.

Our detailed structural and functional analyses have revealed that Arg-44 interacts with the phosphate group of AMP starting with the binary complex (Yan et al., 1990b; Jiang et al., 1991) and that both Arg-138 and Arg-149 play critically important roles in stabilizing the transition state (Yan et al., 1990a,b). The quantitative data and interpretations of our work on these residues differed significantly from those of Kim et al. (1989, 1990). This paper addresses the structural and functional roles of the remainder of these arginine residues, Arg-97 and Arg-132.

Site-specific mutagenesis results of Arg-97 have been reported by others for AKe (Reinstein et al., 1989) and AK1h (from human muscle; Kim et al., 1989, 1990). Unfortunately, the results and interpretations from these groups are again contradicting, which appears to be a common phenomenon for AK as summarized in our recent review (Tsai & Yan, 1991). Reinstein et al. (1989) reported an 85-fold increase in the $K_m$ of AMP and an 88-fold decrease in the $k_{cat}$ of the R88G mutant of AKe (R88 in AKe corresponds to R97 in AK1) and suggested that "it possibly stabilizes the transferable $\gamma$-phosphate group from ATP to AMP in the transition state". Kim et al. (1989, 1990), on the other hand, reported only very small changes in the $K_m$ of both AMP and MgATP and a 50–85-fold decrease in the $k_{cat}$ of the R97A mutant of AK1h. Thus, even though the effects on $k_{cat}$ are similar, the perturbations in $K_m$ are drastically different between the two cases, and the functional roles of Arg-97 remain to be established.

The functional roles of Arg-132 have only been reported for AK1h by Kim et al. (1990): substitution of Arg-132 by alanine led to an 18-fold increase in the $K_m$ of MgATP, a 13-fold increase in the $K_m$ of AMP, and a 13 000–28 000-fold decrease in $k_{cat}$. Such results led the authors to conclude that "Arg-132 would appear to be an essential residue for catalysis, interacting largely with MgATP and only partially with AMP".

A potential problem in the previous studies is that the $k_{cat}$ and $K_m$ values reported in these papers (Kim et al., 1989, 1990; Reinstein et al., 1989) were only apparent values since one of the substrates was held at a constant but not necessarily saturating concentration. The structural characterization of the mutant enzymes in these reports was also limited to techniques with relatively low resolution.

We report evaluation of the structural and functional roles of Arg-97 and Arg-132 by site-directed mutagenesis in conjunction with one- and two-dimensional proton NMR, kinetics, and guanidine hydrochloride-induced denaturation. In addition, the reaction of adenosine 5′-monothiophosphate (AMPS) and MgATP was compared for WT and R97M by $^{31}P$ NMR spectroscopy to evaluate the contribution of Arg-97 to the phosphorus stereospecificity of AK. The results indicate that substitution of methionine at position 132 destabilizes the transition state by several kilocalories per mole but exhibits little effect on the binding affinity as opposed to the result of Kim et al. (1990). R97M yields a dramatic and site-specific effect on AMP binding, which agrees with that of Reinstein et al. (1989) and disagrees with that of Kim et al. (1989, 1990). Furthermore, the stereospecificity results provide strong evidence toward the interaction of Arg-97 with the phosphoryl moiety of AMP and demonstrate the feasibility of manipulating phosphorus stereospecificity of an enzyme by site-directed mutagenesis. Part of the results with Arg-97 have been described in a preliminary communication (Dahnke et al., 1991).

## Materials and Methods

*Materials.* Oligonucleotides were purchased from Research Genetics and the Biochemical Instrument Center of The Ohio State University. DNA sequencing and mutagenesis kits were obtained from U.S. Biochemicals and Amersham, respectively. ADP, AMP, AMPS, ATP, and coupling enzymes were obtained from Sigma. Other phosphorothioate analogues were synthesized as described below. Guanidine hydrochloride (Gdn-HCl) was purchased from Calbiochem and used without further purification. Perdeuterated Tris was obtained from MSD Isotopes. All other chemicals were of reagent grade.

*Synthesis of Phosphorothioate Analogues.* The single isomers ($R_p$)- and ($S_p$)-adenosine 5′-(1-thiotriphosphate) (ATP$\alpha$S), as well as the mixture ($R_p$,$S_p$)-adenosine 5′-(1-thiodiphosphate) (ADP$\alpha$S), were synthesized by the methods of Eckstein and Goody (1976). The single isomers ($R_p$)- and ($S_p$)-ADP$\alpha$S were synthesized as described by Sheu and Frey (1977). These compounds were characterized by $^{31}P$ chemical shifts (Sheu & Frey, 1977; Jaffe & Cohn, 1978) and HPLC retention factors (Sammons, 1982).

*Construction and Purification of Mutants.* The oligonucleotides used for construction are as follows: R97M, GGCTACCCT*AT*GGAGGTGAAG; R132M, CTGCTGAAG*AT*GGGAGACC. The mutants were constructed by the method of Eckstein and co-workers (Taylor et al., 1985a,b) using an Amersham mutagenesis kit. Subcloning and sequencing of the AK gene from the original R97M enzyme indicated that it was a double mutant,



R97M/R149S. Upon this finding, the single mutant at position 97 was reconstructed from the WT gene as described above. R97M was purified and assayed as described by Tian et al. (1988), except for a 0–300 mM linear NaCl gradient which was used for elution of the phosphocellulose column. R132M exhibited weak binding to the phosphocellulose resin and was consequently purified by Blue Sepharose and Sephadex G-100 gel filtration chromatography. At this stage, endogenous *E. coli* AK was removed by fast performance liquid chromatography (FPLC) using a phenyl-Sepharose CL-4B hydrophobic column, preequilibrated with a buffer consisting of 30 mM Tris, 1 mM DTT, 1.8 M $(NH_4)_2SO_4$, and 1 mM EDTA, pH 7.7. The pure enzyme was eluted with a 1.0–0 M $(NH_4)_2SO_4$ gradient in 30 mM Tris, 1 mM DTT, and 1 mM EDTA, pH 7.7, and treated as described by Tian et al. (1988). The purity of each preparation was checked by SDS–PAGE with silver staining on a PhastSystem.

*Proton NMR Methods.* Proton NMR experiments were performed on Bruker AM-500 NMR spectrometers. Chemical shifts were referenced to internal sodium 3-(trimethylsilyl)-propionate-2,2,3,3-$d_4$. One- and two-dimensional NMR experiments, sample preparation, and titration procedures were essentially the same as previously described (Yan et al., 1990b). Briefly, the buffer was composed of 20 mM perdeuterated Tris, 65 mM KCl, 2 mM DTT, and 0.5 mM EDTA, pH 7.8 (pH meter reading without correcting for deuterium isotope effects). The enzyme concentrations were about 1 mM for 1D NMR experiments and 2.5 mM for 2D NMR experiments, and the temperature was 27 °C. For 2D NMR, standard pulse sequences and phase cycling were used for NOESY experiments (Bodenhausen et al., 1984), with a mixing time of 200 ms. The sweep widths were 11.5 ppm. A 2048 × 400 matrix in time domain was recorded and zero-filled to a 4096 × 1024 matrix prior to multiplication by a Gaussian function (LB = −3, GB = 0.1) and Fourier transformation.

*Phosphorus NMR Methods.* P-31 NMR experiments were performed on Bruker AM-250 and 300 NMR spectrometers at 30 °C. All chemical shifts were referenced to external 85% $H_3PO_4$. All spectra were broadband decoupled with the WALTZ sequence. The spectral width was 75 ppm, and 16-32 data points were recorded for each spectrum in the quadrature detection mode. A 45° pulse and a 0–1.0-s relaxation delay were used. Acquisition times ranged from 1.5–2.0 s, repetition times were 2.0–2.5 s, and 1000–23 000 transients were obtained. A 0.5–2.0-Hz line broadening was applied to the time domain data prior to Fourier transformation. Unless otherwise noted, only the regions of the $P_\alpha$ resonances are shown in the spectra.

*Assignment and Quantitization of Isomers.* The assignment of components within the reaction mixture was accomplished by addition of known isomers to the sample, whose relative chemical shifts are in agreement with those reported previously (Sheu & Frey, 1977; Jaffe & Cohn, 1978). It should be noted that the chemical shift values of thiophosphate resonances are extremely sensitive to pH and magnesium ion concentration (Jaffe & Cohn, 1978). As a result, minor differences in chemical shift for the same species may occur as the sample conditions differ slightly from reaction to reaction. The intensities of various components described in the text have been measured by cutting and weighing from greatly expanded spectra.

*Steady-State Kinetics.* The kinetic experiments were carried out by monitoring ADP formation with pyruvate kinase/lactate dehydrogenase as the coupling system (Rhoads & Lowenstein, 1968). The details have been described previously (Tian et al., 1988). The kinetic parameters were obtained by varying both AMP and MgATP concentrations and the data analyzed according to Cleland (1986):

$$v = \frac{ABV}{K_aK_{ib} + K_bA + K_aB + AB}$$

where $v$ is the reaction rate, the subscripts a and b represent the two substrates MgATP and AMP, respectively, $A$ and $B$ are the concentrations of the corresponding substrates, and $V$ is the maximum velocity. The $K$ and $K_i$ values (Michaelis and dissociation constants, respectively) obtained from such analysis were compared to the $K_m$ and $K_d$ values, respectively, measured by saturating one substrate ($K_m$) and by titration studies with NMR ($K_d$) (Tian et al., 1990; Sanders et al., 1989). Although the values were comparable for R132M, $K_i$ and $K_d$ (estimated) deviated substantially for R97M.

*Gdn-HCl-Induced Denaturation.* The reversible denaturation of the enzymes by Gdn-HCl was followed by monitoring the ellipticity at 222.0 nm of CD spectra obtained with a JASCO J-500C polarimeter. The exact concentration of a stock solution of Gdn-HCl in distilled $H_2O$ was calculated from the refractive index (Nozaki, 1972). A 10× stock solution of Tris and KCl (pH 8.0) was added to a final concentration of 75 mM Tris and 65 mM KCl, and the concentration of Gdn-HCl was corrected for dilution effects. Further pH adjustments were usually not required. A 1–4 mM stock solution of enzyme was prepared by dissolving the enzyme in a buffer consisting of 75 mM Tris, 65 mM KCl, and 1 mM DTT, pH 8.0. Precipitate was removed by centrifugation at 15000$g$ for 5 min. Components were mixed in a quartz cuvette of pathlength 10 mm in the order of enzyme, buffer, and Gdn-HCl and allowed to equilibrate at 25 °C for 10 min. Spectra were baseline corrected.

## Results

*Kinetic Properties of Mutants.* The steady-state kinetic data of WT, R97M, and R132M are listed in Table I. The data indicate that replacement of positively charged arginine with uncharged methionine at position 132 results in a dramatic decrease in $k_{cat}$ by a factor of $8.0 \times 10^3$. This magnitude of change in $k_{cat}$ is comparable to that of the R132A mutant of AK1h reported by Kim et al. (1990). However, contrary to their report of substantial increases in $K_m$, we observed no significant differences in the dissociation and Michaelis constants ($K_i$ and $K$, respectively) for AMP or MgATP. Kinetic analysis of R97M resulted in 6- and 28-fold increases in $K_i$ and $K$ of AMP, respectively, with no significant perturbation in MgATP binding and a moderate (30-fold) decrease in $k_{cat}$. The specific binding effect on AMP agrees with the result of Reinstein et al. (1989) and contradicts that of Kim et al. (1989, 1990). Also listed in Table I are the kinetic data of a double mutant, R97M/R149S. This mutant enzyme was obtained incidentally in our first construction of the R97M mutant. The catalytic activity of R97M/R149S is so low that only a rough estimation could be obtained.

*Conformational Stability of WT and Mutants.* The free energy of unfolding, $\Delta G_d^{H_2O}$, a measure of the conformational stability of an enzyme, was determined by monitoring the change in ellipticity of the CD spectra with varying concentrations of Gdn-HCl. This method differs from the previous UV method used in this laboratory (Tian et al., 1988), as it has been found to be more sensitive and to require less enzyme than UV difference spectroscopy. The results, shown in Table II, clearly indicate that the conformational stabilities of R132M, R97M, and R97M/R149S do not differ significantly

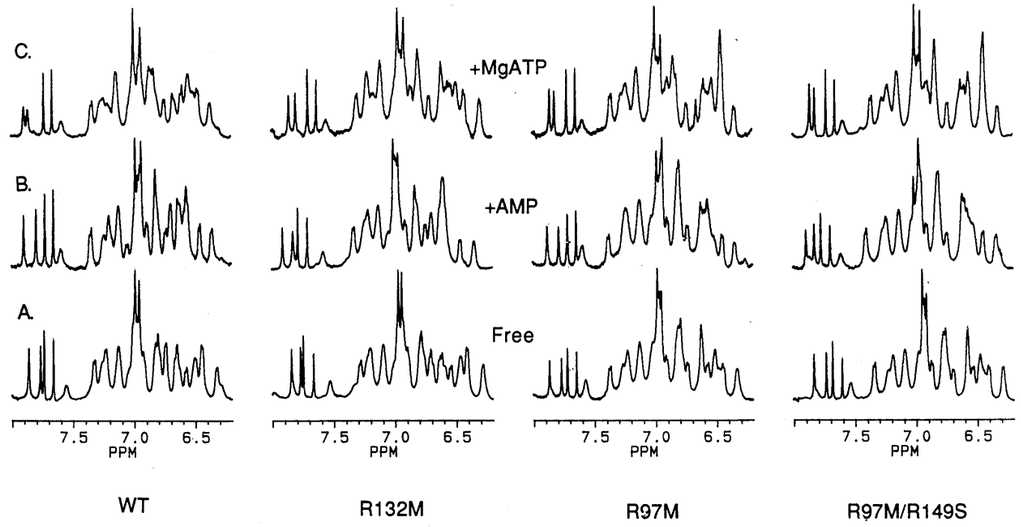


FIGURE 2: One-dimensional proton NMR spectra of the aromatic protons of WT (far left), R132M (left), R97M (right), and R97M/R149S (far right) as free (A), AMP complexed (B), and MgATP complexed (C). The spectra of WT are reproduced from Sanders et al. (1989). All spectra were obtained at pH 7.8, 27 °C, and the FIDs were processed with a 1-Hz line broadening. The concentrations of free enzymes are ca. 1 mM for all cases. The millimolar concentrations of AK/AMP are 1.2/3.4 R132M, 1.0/10.7 R97M, and 0.9/10.5 R97M/R149S; the millimolar concentrations of AK/ATP/$Mg^{2+}$ are 0.9/7.0/8 R132M, 0.8/4.9/11 R97M, and 0.4/5.7/12 R97M/R149S. Due to the low affinity of R97M and R97M/R149S, these two mutants may not be saturated by AMP even with a 10-fold excess of AMP.

Table I: Summary of Steady-State Kinetic and Binding Data for WT, R132M, R97M, R149M, and R97M/R149S[a]

| parameter | unit | WT[b] | R132M | R97M | R149M[c] | R97M/R149S |
|---|---|---|---|---|---|---|
| | | | Steady-State Kinetics | | | |
| $k_{cat}$ | ($s^{-1}$) | 650 | 0.083 ($1.3 \times 10^{-4}$) | 22 (0.034) | 0.42 ($6.5 \times 10^{-4}$) | ≤0.003 ($4.6 \times 10^{-6}$) |
| $K_{(MgATP)}$ | (mM) | 0.042 | 0.056 | 0.083 | 5.6 (130) | |
| $K_{(AMP)}$ | (mM) | 0.098 | 0.053 | 2.78 (28) | 12.4 (130) | |
| $k_{cat}/K_{(MgATP)}$ | ($s^{-1}$ $M^{-1}$) | $1.55 \times 10^7$ | $1.5 \times 10^3$ ($1.0 \times 10^{-4}$) | $0.26 \times 10^6$ (0.017) | 0.29 | |
| $k_{cat}/K_{(AMP)}$ | ($s^{-1}$ $M^{-1}$) | $0.66 \times 10^7$ | $1.6 \times 10^3$ ($2.4 \times 10^{-4}$) | $7.9 \times 10^3$ ($1.2 \times 10^{-3}$) | 0.64 | |
| $K_{i(MgATP)}$ | (mM) | 0.16 | 0.18 | 0.066 | 75 ($4.8 \times 10^{-6}$) | |
| $K_{i(AMP)}$ | (mM) | 0.37 | 0.17 | 2.22 (6) | 34 ($5.1 \times 10^{-6}$) | |
| | | | Titration Experiments with NMR | | | |
| $K_{d(MgATP)}$ | (mM) | 0.17 | 0.52 | 0.08 | 0.26 | 0.18 |
| $K_{d(AMP)}$ | (mM) | 0.50 | 0.36 | | | |

[a] The kinetic data were obtained by varying concentrations of both substrates. Numbers in parentheses indicate the ratios between the mutant and WT. [b] The kinetic data for WT are from Tian et al. (1990); the $K_d$ values for WT are from Sanders et al. (1989). [c] The kinetic data and $K_d$ value for R149M are from Yan et al. (1990b).

Table II: Summary of Conformational Stabilities for WT, R132M, R97M, and R97M/R149S[a]

| parameter | unit | WT | R132M | R97M | R97M/R149S |
|---|---|---|---|---|---|
| $\Delta G_d^{H_2O}$ | (kcal/mol) | 4.5 | 5.2 | 5.7 | 5.1 |
| $m$ | [kcal/(mol·M)] | 5.7 | 5.9 | 6.5 | 6.2 |

[a] Determined by monitoring guanidine hydrochloride-induced unfolding with circular dichroism, using the equation $\Delta G_d = \Delta G_d^{H_2O} - m$[Gdn-HCl] where $\Delta G_d$ is the Gibbs free energy change at various concentrations of Gdn-HCl, $\Delta G_d^{H_2O}$ is the Gibbs free energy change at zero concentration of Gdn-HCl, and $m$ is a constant (Pace et al., 1986).

from that of the native enzyme.

*Proton NMR Analysis of Free and Substrate-Bound Mutants.* One potential pitfall of site-directed mutagenesis is structural changes and contributions they may make (if any) to perturbations in function. As demonstrated by our previous work, it is necessary to study conformations of mutants in both free and substrate-bound forms before the kinetic data can be interpreted quantitatively. For R132M and R97M, this conformational characterization was achieved by proton NMR comparisons with WT AK. Figure 2 shows the spectra of the aromatic protons of WT AK, R132M, R97M, and R97M/R149S as free (A), AMP (B), and MgATP complexed (C). The spectra of R132M are quite similar to those of WT for the free form, but they exhibit slight differences in the AMP and the MgATP complexes. Mutagenesis at position 97 appears to perturb the spectra in the range 6.4–6.8 ppm for the free form and the two binary complexes. It should be noticed, however, that the "AMP complexes" for R97M and R97M/R149S in Figure 2 may not represent the fully complexed forms due to the weak affinity of these two mutants for AMP as described in a later section.

*Proton NMR Analysis of $MgAP_5A$ Complexes of Mutants.* To further evaluate the extent of structural changes observed for the mutant enzymes, we examined the complexes R132M·$MgAP_5A$ and R97M/R149S·$MgAP_5A$ by 1D and 2D NMR. Since these complexes are likely to have more extensive perturbations than the free enzymes and the binary complexes, one need not be concerned with perturbations in the latter if the structural perturbations in these complexes are not extensive. The same rationale lies behind the use of the double mutant instead of R97M. As seen in Figure 3, the perturbations in the 1D spectra of the $MgAP_5A$ complexes are also



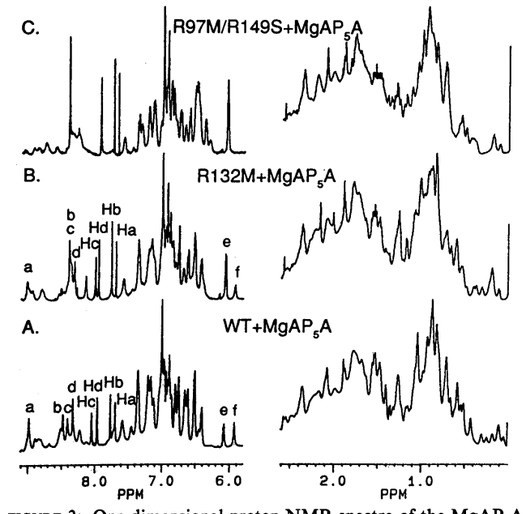


FIGURE 3: One-dimensional proton NMR spectra of the $MgAP_5A$ complexes of WT (A), R132M (B), and R97M/R149S (C). Peaks a–f are due to bound $MgAP_5A$: $H_2$(I) (a); $H_8$(I) (b); $H_8$(II) (c); $H_2$(II) (d); $H_{1'}$(II) (e); $H_{1'}$(I) (f). The spectrum of WT is reproduced from Yan et al. (1990b). The millimolar concentrations of AK/$AP_5A$/$Mg^{2+}$ are 2.0/3.0/3.0 (B) and 2.0/4.0/4.0 (C). The FIDs were processed with Gaussian multiplication (LB = −5, GB = 0.1). Intermediate exchange rates for spectrum B cause signal broadening and overlap of peaks b and c. It should be noted that the $H_8$(free) and $H_{1'}$(free) resonances in spectrum B overlap $H_8$(II) and $H_{1'}$(II) resonances, respectively, whereas $H_2$(free) resonates at 8.19 ppm. The three sets of adenosine resonances of bound and free forms are exchange-averaged beyond separation in spectrum C.

small, but they are somewhat more extensive than those observed for the binary complexes. The peaks arising from $H_{1'}$, $H_2$, and $H_8$ of $AP_5A$ (peaks a–f, assigned from NOESY spectra) differ only slightly between spectra A and B. The enzyme resonances of A and B differ more extensively in the regions of 0–0.9 ppm and 6.4–6.9 ppm.

For interpretation of whether differences in enzyme resonances reflect local or global conformational changes, NOESY spectra are compared between WT and R132M as shown in Figure 4 (panels A and B, respectively). A close analysis of the spectra reveals only minor differences in the pattern of aromatic–aromatic and aromatic–aliphatic cross-peaks. The chemical shifts of the aromatic spin systems have been partially assigned from the 1D and NOESY spectra in analogy to the assignment of WT·$MgAP_5A$ (Yan et al., 1990a) and are listed in Table III. There are only four aromatic resonances which differ (>0.02 ppm) in chemical shift: Fa, 0.06 ppm; Fd, 0.03 ppm; Ye and Hc (His-36), 0.04 ppm. Large differences in Fa have been previously observed (Sanders et al., 1989; Yan et al., 1990a,b) and reflect the sensitivity of this resonance to mutagenesis. The other differences represent minimal changes in the structure. Overall, the differences in the 1D and 2D spectra of the $MgAP_5A$ complexes between R132M and WT, like those of R138M and R149M, are more extensive than those of the binary complexes, yet they are minor and indicative of localized rather than global conformational changes. This result, coupled with the NMR binding studies described in the next section, will allow a quantitative analysis of the kinetic data for R132M.

Also shown in Figure 3 is the 1D spectrum of the complex of $MgAP_5A$ with the double mutant R97M/R149S. There is evidence that $MgAP_5A$ is bound with weaker affinity to the double mutant, since the adenosine protons ($H_8$, $H_2$ and $H_{1'}$), free and the two sets of bound, have exchange-averaged to only one set of signals. The 2D NOESY spectrum of the complex (Figure 4C) again indicates that the aromatic–aromatic and aromatic–aliphatic enzyme cross-peaks have a similar pattern to WT and consequently a conservation in tertiary structure. Comparison of the assignment of the aromatic resonances with WT (Table III) reveals that only two resonances differ significantly with WT: Fa, 0.13 ppm; Hc, 0.09 ppm. The sub-

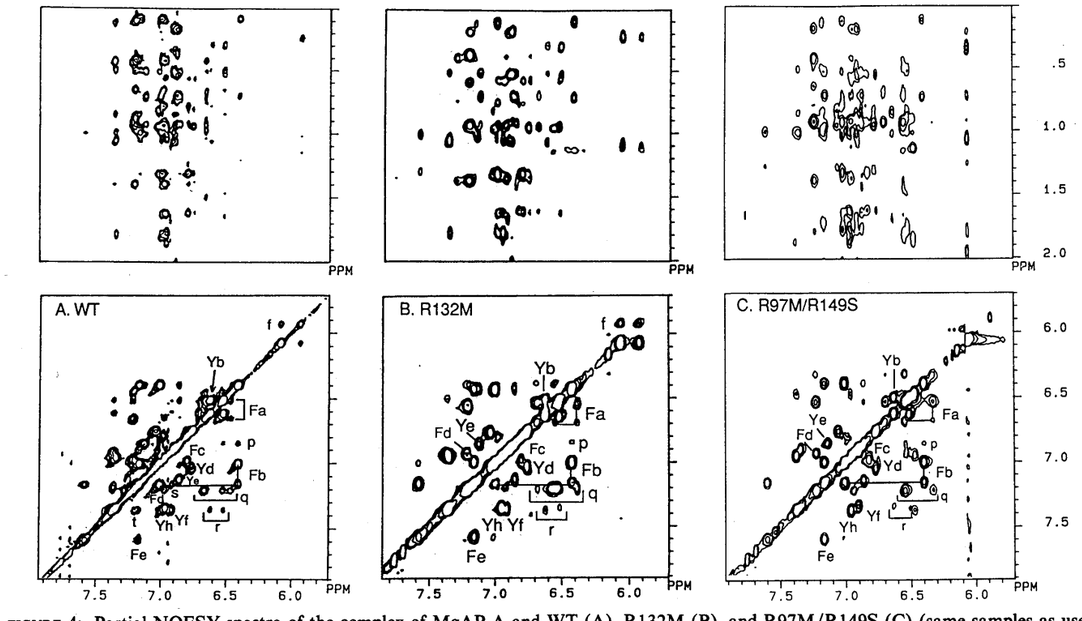


FIGURE 4: Partial NOESY spectra of the complex of $MgAP_5A$ and WT (A), R132M (B), and R97M/R149S (C) (same samples as used for Figure 3). The cross-peak f arises from exchange between the two $H_{1'}$ protons of bound $MgAP_5A$, while cross-peaks p–t arise from interresidue NOEs, as described previously (Yan et al., 1990a,b); cross-peaks s and t are not detectable for (B) or (C).

Table III: Chemical Shifts of the Aromatic Residues of the $MgAP_5A$ Complexes (pH 7.8)[a]

| spin system | R132M·$MgAP_5A$ | | | R197M/R149S·$MgAP_5A$ | | |
|---|---|---|---|---|---|---|
| Fa | 6.38 (−0.06) | 6.52 | 6.68 (+0.03) | 6.31 (−0.13) | 6.53 | 6.67 |
| Fb | 6.42 | 7.00 | 7.16 | 6.38 | 7.00 | 7.14 |
| Fc[b] | 6.80 | 6.97 | | 6.80 | 6.98 | |
| Fd[b] | 6.94 (−0.03) | 7.20 | | 6.92 (−0.05) | 7.21 | |
| Fe | | 7.15 | 7.57 | | 7.15 | 7.58 |
| Yb | 6.51 | 6.62 | | 6.50 | 6.61 | |
| Yd | 6.75 | 7.03 | | 6.75 | 7.03 | |
| Ye | 6.84 (−0.04) | 7.11 | | 6.85 (−0.03) | 7.12 | |
| Yf | 6.92 | 7.36 | | 6.88 (−0.04) | 7.32 (−0.04) | |
| Yh | 6.96 | 7.35 | | 6.96 | 7.35 | |
| Ha | 7.00 | 7.69 | | 7.00 | 7.67 | |
| Hb | 6.92 | 7.75 | | 6.92 | 7.74 | |
| Hc | | 8.00 (−0.04) | | | 7.95 (−0.09) | |
| Hd | 6.75 | 7.94 | | | 7.94 | |

[a] The underlined are the resonances which differ by >0.02 ppm from the corresponding resonances of WT·$MgAP_5A$, and the magnitudes of the differences are shown in parentheses. [b] Fc and Fd correspond to Xa and Xb, respectively, of the WT spin systems in previous reports (Yan et al., 1990a,b).

stantial shift of Fa can be expected for this double mutant on the basis of the previous demonstrations of the sensitivity of this aromatic residue. We have also detected differences of Hc (His-36) with R128A, R138K, and R149M (Yan et al., 1990a,b). It is quite remarkable that a double mutant, in which two conserved residues have been changed, remains conformationally intact. These results suggest that the kinetic data of R132M and R97M can be interpreted with confidence, as described in the Discussion.

*Analysis of Substrate Binding Affinity by NMR Titration.* Another technique used to evaluate the impact of structural perturbations introduced by mutagenesis, as well as to confirm dissociation constants derived from kinetic analysis, is NMR substrate titration. The dissociation constants of MgATP and AMP for R132M (Table I) determined from such experiments are 0.52 and 0.36 mM, respectively, which are comparable to the corresponding $K_i$ values obtained from kinetics and the corresponding $K_d$ values from the NMR experiments of WT AK, as listed in Table I. These data support the lack of changes in the $K_i$ values of R132M determined from kinetics.

For R97M, the kinetic data for AMP binding show a relatively small (6-fold) increase in $K_i$, although the Michaelis constant increases nearly 30-fold. However, NMR titrations with AMP indicate that binding affinity for the binary complex is very weak for this mutant. As illustrated in Figure 5, the characteristic upfield shift of the aromatic resonance Fa and downfield shift of the adenine $H_2$ for the binary complex, clearly observed for WT, are much less pronounced in the corresponding experiment with R97M. Nonlinear least-squares fitting of the data to obtain binding constants is quite difficult in this case since the affinity of AMP for the AMP site could be comparable to or even weaker than the affinity of AMP for the MgATP site (ca. 4.3 mM; Sanders et al., 1989). However, the binding affinity observed with this titration (as judged by the concentration range of substrate required to affect the AMP-sensitive resonances) is comparable to that of R44M, another mutant AK with a selective and dramatic effect on AMP binding (20–30-fold increases in binding constants; Yan et al., 1990b). These data indicate 3–4-fold differences between the estimate $K_d$ (from NMR) and $K_i$ (from kinetics) for R97M. The specific reason behind such differences is unknown, but it could be due to slight deviation of the mutant from the rapid equilibrium random bi-bi mechanism exhibited by WT (Rhoads & Lowenstein, 1968; Tsai & Yan, 1991). As predicted from the kinetic data, the perturbation in AMP binding is not carried over into the MgATP site, since titrations with the latter substrate were

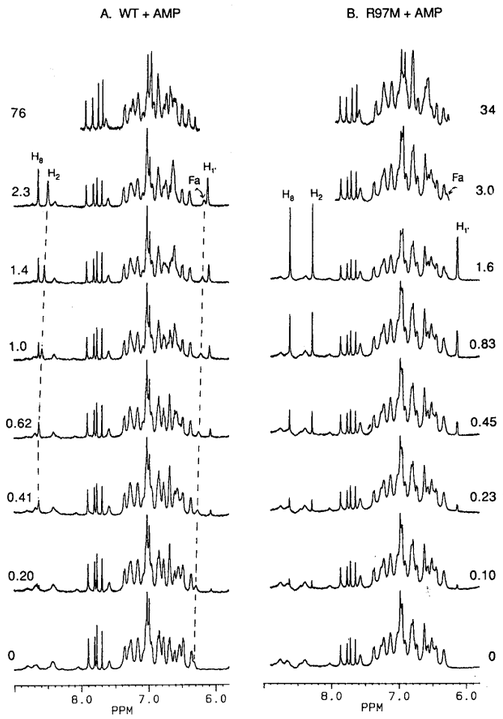


FIGURE 5: Proton NMR titration of WT (A) and R97M (B) with AMP. The ratios [AMP]/[AK] are shown, and the starting concentration of free enzyme is approximately 1 mM for both samples. The labeled peaks $H_8$, $H_2$, and $H_{1'}$ are AMP resonances, whereas Fa is from a phenylalanine. The FIDs have been processed with 1-Hz line broadening, and those of WT are reproduced from Sanders et al. (1989).

quite similar to those of the WT and afforded comparable dissociation constants (Table I).

While the binding affinities of R97M/R149S toward substrates were not measurable from kinetics due to the nearly undetectable activity, the NMR titration experiments (Figure 6) showed that this double mutant has lost its capability for AMP binding almost entirely (>50-fold increase in $K_d$, to the best of our estimation) while the MgATP binding capability remains nearly intact. This is perhaps the most interesting of all results reported in this paper, and it strongly supports



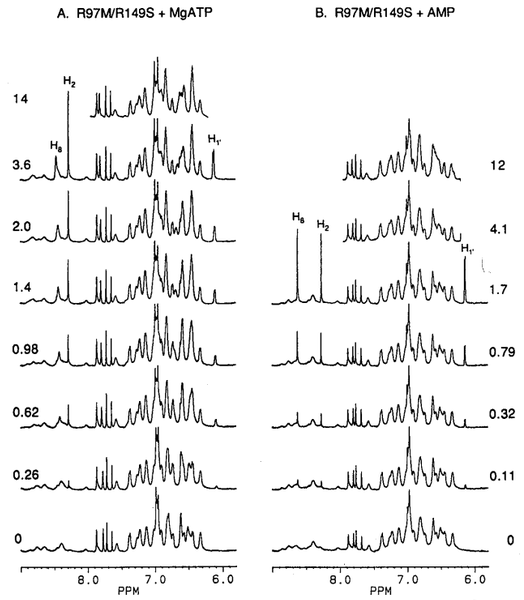


FIGURE 6: Proton NMR titration of the double mutant R97M/R149S with MgATP (A) and AMP (B). The ratios [MgATP]/[AK] (A) and [AMP]/[AK] (B) are shown, and the starting concentration of free enzyme is approximately 1 mM for both samples. The labeled peaks $H_8$, $H_2$, and $H_{1'}$ are MgATP resonances (A) and AMP resonances (B). The FIDs have been processed with 1-Hz line broadening.

the independence of the two binding sites.

*How Does Arginine-97 Interact with AMP*? The results of kinetic and NMR analyses allowed us to conclude that Arg-97 interacts specifically with AMP, but they provide no information about the nature of the interaction. The crystal structure of the AK3·AMP complex (Diederichs & Schulz, 1990, 1991) indicates that the guanidinium groups of Arg-41 and Arg-92 (Arg-44 and Arg-97 in muscle AK) point toward the phosphoryl group from opposing directions. We have previously demonstrated that R44M completely reverses stereospecificity at the AMP site in the reaction of AMPS with MgATP (Jiang et al., 1991). We therefore predicted that the stereospecificity results of R97M should act contrary to R44M and *enhance* the stereospecificity of the WI reaction. Such a prediction, if observed, will serve as an independent and strong evidence that Arg-97 interacts with the phosphoryl group of AMP.

*Confirmation of Wild-Type AK Phosphorus Stereospecificity.* As a first step toward manipulating the stereospecificity of AK by site-directed mutagenesis, the specificity of chicken muscle at both binding sites was established and compared to that of other variants of AK. The reaction of MgATP and AMPS catalyzed by WT AK was followed by $^{31}P$ NMR spectroscopy, and a representative spectrum is shown in Figure 7A. This reaction clearly affords one predominant isomer of ADPαS, which was subsequently assigned as $S_p$ by the addition of known isomers. The newly formed $(S_p)$-ADPαS is readily converted to $(S_p)$-ATPαS at the MgATP site, suggesting that the preferred configuration at the $P_\alpha$ position of MgATP is also $S_p$. Thus, the stereospecificity of chicken muscle AK at both sites is consistent with previously-established stereospecificities of AK from other sources (Eckstein & Goody, 1976; Kalbitzer et al., 1983; Sheu & Frey, 1977; Tomasselli & Noda, 1981). For the purpose of discussion, the result of R44M is shown in Figure 7B, which indicates reversal

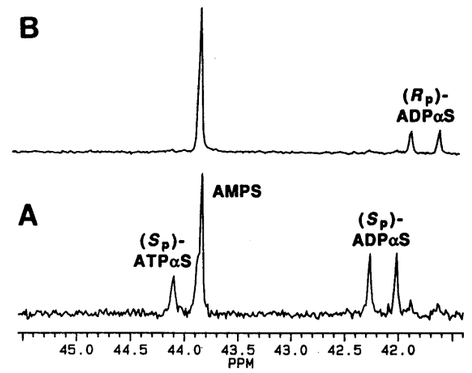


FIGURE 7: $^{31}P$ NMR spectra showing the stereospecificity of WT (A) and R44M (B). The right half of the doublet of $(S_p)$-ATPαS overlaps with the singlet of AMPS. The position of $(R_p)$-ATPαS should be upfield from AMPS. The starting reaction mixture (2 mL) consisted of 22 mM AMPS, 75 mM ATP, 45 mM $Mg(NO_3)_2$, and ca. 40 μg of WT or ca. 400 μg of R44M, in a 50 mM Tris buffer containing 50 mM KCl and 2.5 mM EDTA, pH 7.8. This spectrum was obtained in the absence of a deuterium lock.

of stereospecificity at the AMP site [formation of $(R_p)$-ADPαS exclusively] but not at the MgATP site [$(R_p)$-ADPαS was not converted to $(R_p)$-ATPαS] (Jiang et al., 1991).

In Figure 7A, ca. 5% of the $R_p$ isomer can be detected for ADPαS and no $R_p$ isomer is observable for ATPαS. Thus, both sites show a high degree of stereospecificity. However, it is important to note that the degree of stereospecificity revealed by $^{31}P$ NMR is only qualitative and depends on the extent of reaction. Although the observed stereospecificity arises from differences in the thermodynamics of the interactions between active site residues and the two isomers (or conformers), there is little difference in the free energies of the isomers outside of the active site. Thus the observed stereospecificity is a kinetic event, and the ratio of $S_p/R_p$ should eventually reach the equilibrium value of ca. 1 upon prolonged reaction.

*Enhancement of AMP Site Stereospecificity with R97M.* Since the ratio of $R_p/S_p$ in the product ADPαS depends on the extent of reaction of AMPS as noted above, verification of an enhanced stereospecificity requires the demonstration that the ratio $R_p/S_p$, or the percentage of $R_p$ in the total phosphorothioate species in the reaction mixture, is smaller at a later stage of the reaction catalyzed by R97M than that at an earlier stage of reaction catalyzed by WT. The reaction mixtures of WT after 9%, 17%, and 29%, respectively, AMPS has been converted to products are shown in panels A–C of Figure 8, respectively. The spectrum of R97M at 27% conversion is seen in Figure 8D. The percentage of $R_p$ in the total phosphorothioate species in the reaction mixture present for the WT reactions is approximately 0.27%, 0.54%, and 1.7% for points A–C, respectively, whereas in spectrum D, $(R_p)$-ADPαS is undetectable. It should be noted that the value of 1.7% for the WT reaction is misleadingly high, since equilibrium has already been previously established. In the absence of a change in stereospecificity, the theoretical percentage of $R_p$ for R97M at 27% conversion will be considerably larger than 0.54%, but less than 1.7%. If we select 1% as a conservative estimate, the amount of $(R_p)$-ADPαS in spectrum D should be 3–4 times the amount present in spectrum A (0.27%) if there was no change in stereospecificity. Since the overall signal to noise ratios of all of these spectra are similar and the signal to noise ratio for $(R_p)$-ADPαS in spectrum A

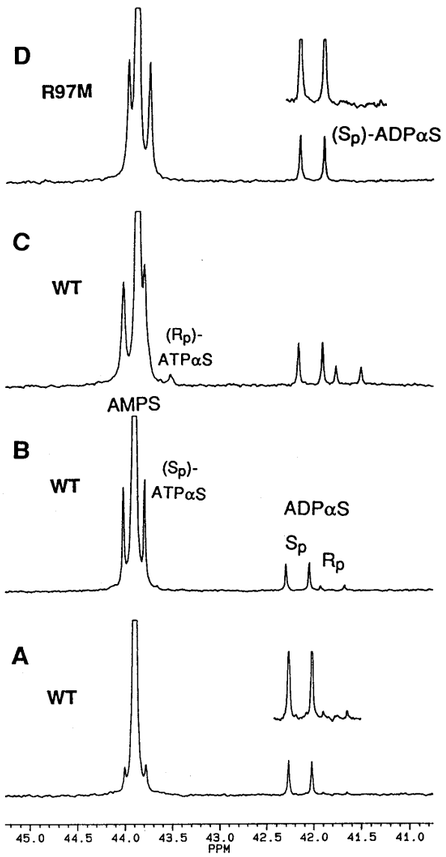


FIGURE 8: $^{31}P$ NMR spectra showing the conversion of AMPS to ADPαS (and subsequent conversion to ATPαS). (A–C) WT AK, after 9%, 17%, and 29%, respectively, of AMPS has reacted; (D) R97M, at 27% conversion. Except for sample C, no ($R_p$)-ATPαS was detectable even in another condition optimized for the detection of ATPαS (spectra not shown). The starting reaction mixture (600 μL) was similar to that of Figure 7, except for the addition of $D_2O$ (final concentration 15%) to the buffer. Spectra A–C were obtained after the addition of 2 μg, 25 μg, and 10 μg of WT, whereas 20 μg of R97M was added in spectrum D. EDTA and triethylamine were added to optimize for the detection of ADPαS. It should be noted that the total reaction time differed considerably for each spectrum.

is ca. 3, the actual amount of ($R_p$)-ADPαS in spectrum D has decreased by at least 10-fold (3 × 3.5). It is therefore concluded that the stereospecificity of R97M has been enhanced by at least 10-fold.

*Confirmation of Stereospecificity of the ATP Binding Site.* For meaningful interpretation of the perturbation of stereospecificity at the AMP site, it is important to show that the perturbation is site-specific, as predicted by the kinetic data. Although we have concluded that the MgATP site prefers the $S_p$ isomer at the $P_\alpha$ position on the basis of Figures 7 and 8, the MgATP site does not have a "fair choice" for isomers in these experiments since only one isomer of ADPαS is formed predominantly. We therefore performed an additional experiment using ($R_p$,$S_p$)-ADPαS. A time course of the reaction with R97M in Figure 9 illustrates the steady removal of ($S_p$)-ADPαS for the formation of ($S_p$)-ATPαS and AMPS, while the $R_p$ isomer remains unreacted. The result indicates that both sites utilize the $S_p$ isomer specifically. As a comparison, we also show that the same experiment with WT gave

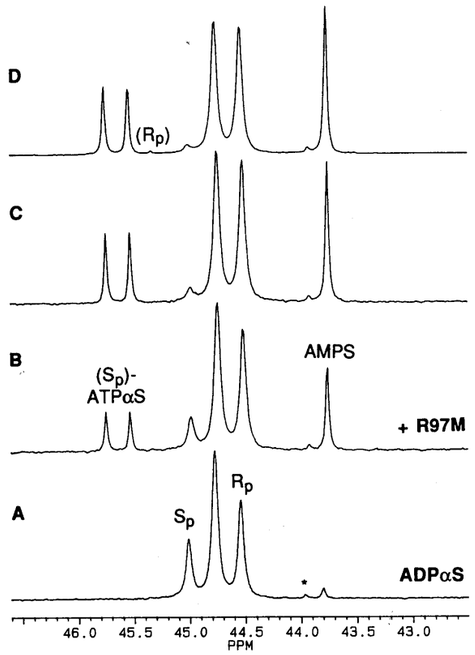


FIGURE 9: Time course of the reaction of R97M and ($R_p$,$S_p$)-ADPαS: (A) ($R_p$,$S_p$)-ADPαS ($R_p$/$S_p$ ca. 4/3); (B) 30 min after the addition of R97M; (C) continuation of (B), 1.5 h; (D) continuation of (C), 72 h. A small amount of ($R_p$)-ATPαS can be detected after prolonged reaction in (D). Sample conditions for the reverse reaction were similar to those of Figure 7, except for the replacement of ATP and AMPS with 22 mM ADPαS. Spectra were obtained after the addition of 25 μg of R97M. The asterisk indicates a small impurity introduced during the synthesis of the phosphorothioate analogues.

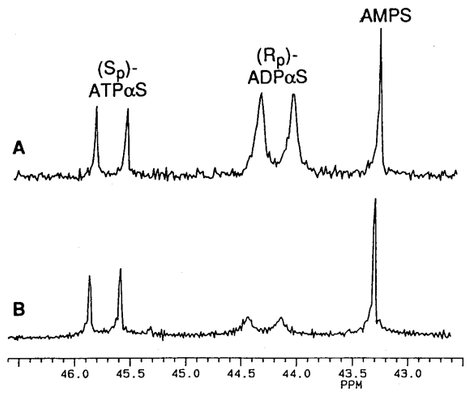


FIGURE 10: Reaction of ($R_p$,$S_p$)-ADPαS catalyzed by WT (A) and R44M (B). Sample conditions for the reactions were similar to those of Figure 9. These spectra were obtained after addition of ca. 20–50 μg of enzyme.

the same result (Figure 10, spectrum A) while the experiment with R44M led to consumption of both isomers (Figure 10B), presumably $R_p$ at the AMP site and $S_p$ at the MgATP site (the small amount of unreacted $R_p$ isomer arises from the slight excess of this isomer in the starting ADPαS). These results establish that the stereospecificity at the MgATP site has not been reversed in any case, but they do not exclude the possibility of an enhancement. Since the degree of stereospecificity at the MgATP site of WT is very high (>99% on the basis of our best estimation), our techniques are not sensitive enough to detect significant enhancement at the MgATP site.





## Discussion

*Arginine-97 Interacts with AMP Starting with the Binary Complex.* The absence of structural perturbation in the double mutant R97M/R149S clearly shows that Arg-97, like the other conserved arginines we have examined, does not contribute significantly to the structural integrity of AK. Free energy calculations indicate that Arg-97 stabilizes AMP by ca. 1–2 kcal/mol starting with the binary complex. Stabilization continues into the ternary complex ($K_m$ effect) and further intensifies at the transition state ($k_{cat}/K_m$ effect). The latter interpretation is justified since we have previously shown that the chemical step is nearly rate-limiting (Tian et al., 1990). The energy contribution at the transition state should be 3.5 kcal/mol according to the relationship $\Delta\Delta G^{\ddagger} = RT \ln [(k_{cat}/K_{iA}K_B)/(k_{cat}'/K_{iA}'K_B')]$, where A and B represent the two substrates.

Our results and interpretations regarding the roles of Arg-97 in AK1c are thus different from those of the same residue in AK1h reported by Kim et al. (1989, 1990); the latter failed to recognize the specific role of this residue toward binding of AMP. While it is possible that the residue plays different roles in the two muscle enzymes, we view this as highly unlikely since (i) these two enzymes should function quite similarly, on the basis of a high average sequence homology among muscle AK of 89% (Schulz, 1987) and (ii) the specific $K_m$ effect on AMP has also been reported for a more distantly related (ca. 31% homology) AK, AKe (Reinstein et al., 1989). On the basis of qualitatively similar kinetic data, however, Reinstein et al. (1989) interpreted that the arginine residue "is involved in binding of AMP or that the two nucleotide sites are tightly coupled" (for the $K_m$ effect) and that "it possibly stabilizes the transferable γ-phosphate group from ATP to AMP in the transition state" (for the $k_{cat}$ effect). We disfavor the role of Arg-97 in interacting with the transferring phosphoryl group and suggest that the decreased $k_{cat}$ for R97M merely reflects the further enhancement of the interaction of Arg-97 with AMP at the transition state. These functional results support the structural observations that Arg-88 of AKy (corresponding to Arg-97 of AK1 or Arg-106 in the systematic numbering system) is in proximity to a phosphate group in the AKy·$MgAP_5A$ complex (Egner et al., 1987) and that Arg-92 of AK3 (corresponding to Arg-97 of AK1) is in contact with the phosphate group of AMP in the AK3·AMP complex (Diederichs & Schulz, 1990, 1991).

It is an interesting exercise to compare the kinetic and structural differences between R97M and R97M/R149S. We already know from previous work that Arg-149 is critical for transition-state stabilization (see Table I) (Yan et al., 1990b), so the virtually undetectable activity of this double mutant is not at all surprising. Furthermore, structural perturbations observed by 1D NMR analysis in free R97M/R149S are nearly *identical* to those in free R97M, whereas free R149M is structurally identical to WT (Yan et al., 1990b). This indicates that no additional conformational changes have occurred for the double mutant that are not inherently part of either of the single mutants. Finally, the conformational stability (free energy of unfolding) of this double mutant, within experimental error, is the same as that of WT and indicates that a relatively "unstable" enzyme (small $\Delta G_d^{H_2O}$ value) such as AK is not perturbed in stability upon removal of two conserved residues.

*Manipulation of AMP Phosphorus Stereospecificity.* While a vast amount of work has been reported on the stereochemical

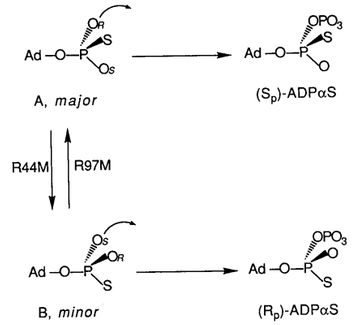


FIGURE 11: Schemes showing the major and minor conformers of AMPS at the active site of WT and the conversion of these conformers to ADPαS. The equilibrium is shifted to conformer B upon R44M mutation and to conformer A upon R97M mutation.

property of the enzyme at the substrate level, little is known about the structural basis of the observed stereospecificity at the enzyme level. In general terms, the specific isomer preferred by the enzyme is the isomer that can fit into the active site and cause the least "pain" (due to replacing an O with S) to the enzyme during the catalytic process The stereospecificity, therefore, is a consequence of the balance of the enzyme–substrate interactions at the active site. A perturbation of such interactions can then be expected to lead to a perturbation in the stereospecificity. The prediction and demonstration of changes in stereospecificity for R97M and R44M (Jiang et al., 1991) have provided strong, irrefutable evidence for the interaction of the arginines and the phosphate during catalysis. In addition, the results have provided further insight into the enzyme–substrate interactions at the active site. As shown schematically in Figure 11, the stereospecificity of WT at the AMP site can be explained by an equilibrium between a major conformer A and a minor conformer B. The equilibrium is shifted toward conformer B in R44M, and toward conformer A in R97M, as indicated by the arrows. We speculate that Arg-44 is more important than Arg-97 in positioning the phosphoryl group during catalysis, since the major conformer is perturbed in the R44M mutant.

*Arginine-132 Is Critical for Transition-State Stabilization.* Although small perturbations in structure have been observed for this mutant in the AMP and the MgATP complexes, as well as 1D and 2D spectra of the $MgAP_5A$ complex, these changes are minor on the basis of the NOESY spectra and the chemical shifts of aromatic spin systems. As seen in Table I, the dissociation constants for AMP and MgATP determined from NMR titration experiments are also comparable to the WT values, and to those derived kinetically.

Having established that Arg-132 does not play a structural role in AK, a quantitative evaluation of kinetics indicates that Arg-132 does play an important role in function as it stabilizes the transition state by 5.1 kcal/mol. This finding places Arg-132 in a group with two other critical transition-state residues, Arg-138 and Arg-149. These three residues have in common large transition-state stabilizations (5.1, 7.0, and 7.3 kcal/mol, for Arg-132, Arg-138, and Arg-149, respectively) and little or no effect on the *binary* complex for either substrate. The effect of stabilization of the *ternary* complex increases in the order Arg-132 < Arg-138 < Arg-149. Interestingly, except for the coalescence of the two adenine $H_8$ resonances, both 1D and 2D NMR spectra of R132M·$MgAP_5A$ are very similar to those of the $MgAP_5A$ complexes of R138K and R149M (Yan et al., 1990a,b). Whereas

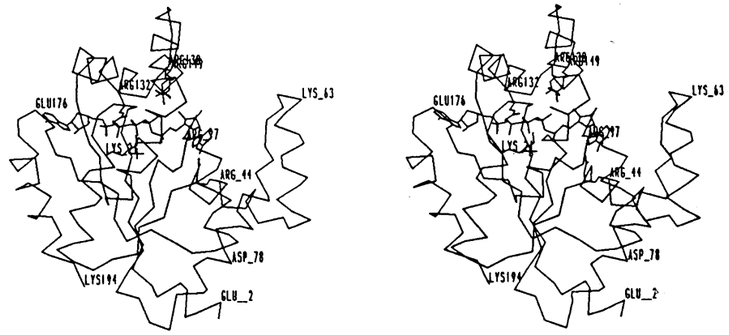


FIGURE 12: Stereoview of the backbone of the 2.1-Å structure of free AK1p (Dreusicke et al., 1988) with side chains of Lys-21, Arg-44, Arg-97, Arg-132, Arg-138, and Arg-149. Using the chain fold overlay of AKy·$MgAP_5A$ and free AK1p as a guide (Egner et al., 1987), $AP_5A$ has been placed into the structure to demonstrate the relationship between the positions of the functionally important side chains in the free enzyme and the possible position of the bisubstrate analogue inhibitor deduced from AKy·$MgAP_5A$.

spectral differences in the R138K and R149M complexes with $MgAP_5A$ are attributed to the $K_m$ effect, i.e., minor conformational changes in the ternary complex as a result of increased $K_m$, no such conclusion can be made with R132M due to the distinct absence of this $K_m$ effect for either substrate.

*Current Status on the Structure–Function Relationship of AK.* The interactions of Arg-44 and Arg-97 with the phosphoryl group of AMP have been well established on the basis of the results presented in this work and pertinent structural and functional studies reviewed by Tsai and Yan (1991). On the basis of the position of the three arginine residues 132, 138, and 149, as well as their functional roles, we have proposed that the side chains of these three arginine residues, possibly in concert with that of Lys-21, surround the transferring phosphate and stabilize the monomeric metaphosphate in case of a dissociative mechanism or the pentacovalent transition state in case of an associative mechanism (Tsai & Yan, 1991). However, such a proposal remains to be verified by further structural studies. Since no crystal structure of a $MgAP_5A$ complex of AK1 is available, we constructed Figure 12 by manually placing $MgAP_5A$ into the structure of free AK1, with side chains of the pertinent residues highlighted. In this model, the "fit" between the four side chains (132, 138, 149, and 21) and the phosphates is not optimal. There are two possible reasons for the discrepancy: (i) The AK1 structure in Figure 12 is that of the free form and does not represent the actual conformation of the complex. A conformational change will definitely bring the arginine side chains closer to the phosphates. However, even in the cocrystal AKy·$MgAP_5A$ the side chain of Arg-149 is not within 3.5 Å of the bound inhibitor (Egner et al., 1987). (ii) The results of AKy (upon which the position of $AP_5A$ in Figure 1 is based) cannot be directly translated into AK1. This is likely since the adenosine moiety at the ATP site in the AKy·$MgAP_5A$ complex is surrounded by a 30-residue "insertion segment" which is absent in AK1 (Egner et al., 1987). In addition, there is some uncertainty regarding which residue in AKy corresponds to the Arg-132 of AK1 (Tsai & Yan, 1991): in the sequence alignment suggested by Schulz (1987), the Arg-132 of AK1 is given a systematic number of 141; in the alignment proposed by Haase et al. (1989), it is 145 (also an arginine). In the former alignment, Arg-128 of AK1 would correspond to residue 137 in systematic numbering (a leucine in AKy and AKe) while in the latter it would correspond to residue 141 (conserved).

*Conclusions.* In light of the results described above, the following important points can be made: (i) Neither Arg-97 nor Arg-132 is required for maintaining the native tertiary structure of AK, as judged by 1D and 2D proton NMR spectra; (ii) the conformational stability of the mutants of both arginines [as well as those of the remaining arginines in the catalytic cleft, see Tsai and Yan (1991)] is identical to WT, and it provides evidence, in conjunction with the NMR data, that the role of these arginines is strictly functional in cytosolic muscle AK; (iii) Arg-132 is critical to stabilization of the transition state, as demonstrated by the dramatic decrease of the $k_{cat}/K_m$ effect of over 5 kcal/mol in the methionine mutant; (iv) Arg-97 affords a selective stabilization of the phosphoryl group of AMP (1–2 kcal/mol), beginning at the stage of the binary complex and continuing into the ternary complex and the transition state (3.5 kcal/mol); and (v) we have been able to manipulate the phosphorus stereospecificity of AK by site-directed mutagenesis.

## Added in Proof

The interpretations in this paper and related earlier papers from our Laboratory are in full agreement with the refined structure of the *E. coli* AK·$AP_5A$ complex which has just appeared (Müller & Schulz, 1992).

## References

Bodenhausen, G., Kogler, H., & Ernst, R. R. (1984) *J. Magn. Reson. 58*, 370–388.
Cleland, W. W. (1986) in *Investigation of Rates and Mechanisms of Reactions Part 1* (Bernasconi, C. F., Ed.), pp 791–870, Wiley, New York.
Dahnke, T., Jiang, R.-T., & Tsai, M.-D. (1991) *J. Am. Chem. Soc. 113*, 9388–9389.
Diederichs, K., & Schulz, G. E. (1990) *Biochemistry 29*, 8138–8144.
Diederichs, K., & Schulz, G. E. (1991) *J. Mol. Biol. 217*, 541–549.
Dreusicke, D., Karplus, A., & Schulz, G. E. (1988) *J. Mol. Biol. 199*, 359–371.
Eckstein, F., & Goody, R. S. (1976) *Biochemstry 15*, 1685–1691.
Egner, U., Tomasselli, A. G., & Schulz, G. E. (1987) *J. Mol. Biol. 195*, 649–658.
Haase, G. H. W., Brune, M., Reinstein, J., Pai, E. F., Pingoud, A., & Wittinghofer, A. (1989) *J. Mol. Biol. 207*, 151–162.
Jaffe, E. K., & Cohn, M. (1978) *Biochemistry 17*, 652–657.
Jiang, R.-T., Dahnke, T., & Tsai, M.-D. (1991) *J. Am. Chem. Soc. 113*, 5485–5486.
Kalbitzer, H. R., Marquetant, R., Connolly, B. A., & Goody, R. S. (1983) *Eur. J. Biochem. 133*, 221–227.



Kim, H. J., Nishikawa, S., Tanaka, T., Uesugi, S., Takenaka, H., Hamada, M., & Kuby, S. A. (1989) *Protein Eng. 2*, 379–386.
Kim, H. J., Nishikawa, S., Tokutomi, Y., Takenaka, H., Hamada, M., Kuby, S. A., & Uesugi, S. (1990) *Biochemistry 29*, 1107–1111.
Kishi, F., Maruyama, M., Tanizawa, Y., & Nakazawa, A. (1986) *J. Biol. Chem. 261*, 2942–2945.
Müller, C. W., & Schulz, G. E. (1988) *J. Mol. Biol. 202*, 909–912.
Müller, C. W., & Schulz, G. E. (1992) *J. Mol. Biol. 224*, 159–177.
Nozaki, Y. (1972) *Methods Enzymol. 26*, 43–50.
Pace, C. N. (1986) *Methods Enzymol. 131*, 266–280.
Reinstein, J., Gilles, A.-M., Rose, T., Wittinghofer, A., Girons, I. S., Bârzu, O., Surewicz, W. K., & Mantsch, H. H. (1989) *J. Biol. Chem. 264*, 8107–8112.
Rhoads, D. G., & Lowenstein, J. M. (1968) *J. Biol. Chem. 243*, 3963–3972.
Sammons, R. D. (1982) Ph.D. Dissertation, The Ohio State University.
Sanders, C. R., II, Tian, G., & Tsai, M.-D. (1989) *Biochemistry 28*, 9028–9043.
Schulz, G. E. (1987) *Cold Spring Harbor Symp. Quant. Biol. 52*, 429–439.
Schulz, G. E., Schiltz, E., Tomasselli, A. G., Frank, R., Brune, M., Wittinghofer, A., & Schirmer, R. H. (1986) *Eur. J. Biochem. 161*, 127–132.
Sheu, K.-F. R., & Frey, P. A. (1977) *J. Biol. Chem. 252*, 4445–4448.
Tanizawa, Y., Kishi, F., Kaneko, T., & Nakazawa, A. (1987) *J. Biochem. (Tokyo) 101*, 1289–1296.
Taylor, J. W., Schmidt, W., Cosstick, R., Okruszek, A., & Eckstein, F. (1985a) *Nucleic Acids Res. 13*, 8749–8764.
Taylor, J. W., Ott, J., & Eckstein, F. (1985b) *Nucleic Acids Res. 13*, 8764–8785.
Tian, G., Sanders, C. R., II, Kishi, F., Nakazawa, A., & Tsai, M.-D. (1988) *Biochemistry 27*, 5544–5552.
Tian, G., Yan, H., Jiang, R.-T., Kishi, F., Nakazawa, A., & Tsai, M.-D. (1990) *Biochemistry 29*, 4296–4304.
Tomasselli, A. G., & Noda, L. H. (1981) *Fed. Proc. 40*, 1864.
Tsai, M.-D. & Yan, H. (1991) *Biochemistry 30*, 6806–6818.
Yan, H., Shi, Z., & Tsai, M.-D. (1990a) *Biochemistry 29*, 6385–6392.
Yan, H., Dahnke, T., Zhou, B., Nakazawa, A., & Tsai, M.-D. (1990b) *Biochemistry 29*, 10956–10964.